Electronic Supplementary Material (ESI) for RSC Advances.

Supporting Information

Nitrogen Doped Graphite Felt Decorated with Porous $Ni_{1.4}Co_{1.6}S_4$ Nanosheets for 3D Pseudocapacitor Electrodes

Xiang Zhang, Yuying Zheng*, Jun Zhou, Wenqing Zheng, Dongyang Chen*

College of Materials Science and Engineering, Fuzhou University, Fuzhou 350116, P. R. China

E-mails: yyzheng@fzu.edu.cn (Y. Zheng); dongyang.chen@fzu.edu.cn (D. Chen)

Table of Contents

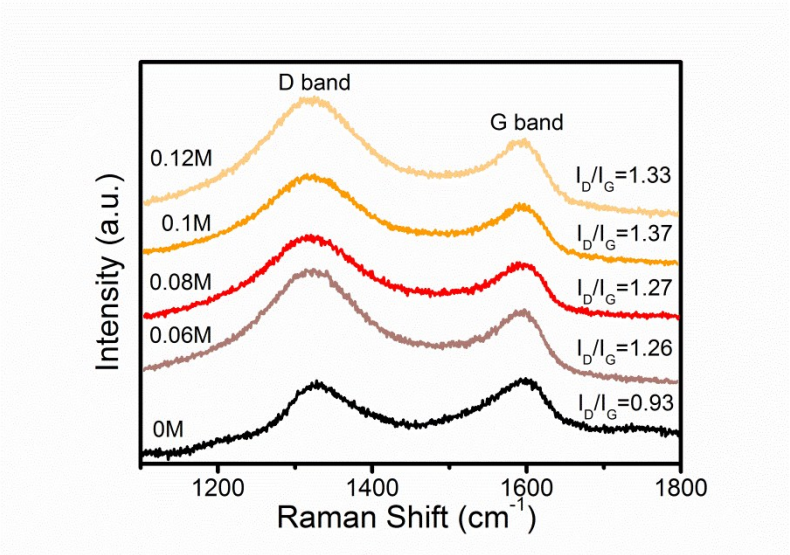

Figure S1. Raman spectroscopy of the NGF-0-900 NGF-0.06-900, NGF-0.08-900, NGF-0.1-900 and NGF-0.12-900. The broad peaks of D band and the highest I_D / I_G value (1.37) of the NGF-0.1-900 indicate a largest degree of defects in NGF-0.1-900 compared to other samples.

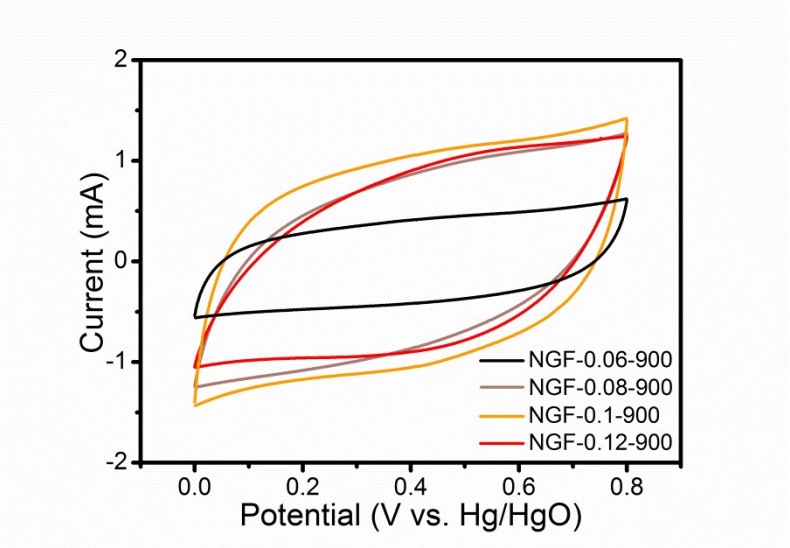

Figure S2. CV curves of the NGF-0.06-900, NGF-0.08-900, NGF-0.1-900 and NGF-0.12-900. The largest enclosed area of the NGF-0.1-900 represents highest capacity.

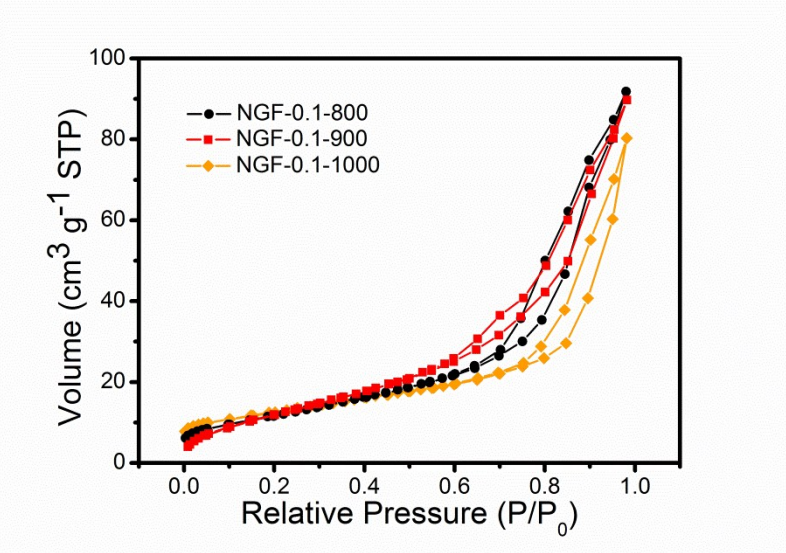

Figure S3. Nitrogen adsorption-desorption isotherm of the NGF-0.1-800, NGF-0.1-900 and NGF-0.1-1000. The hysteresis loops suggest the mesoporous property of all samples.

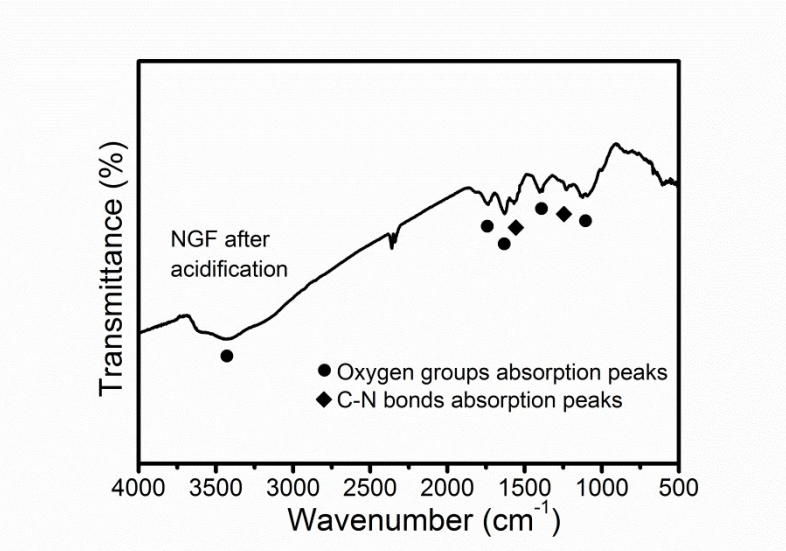

Figure S4. FT-IR spectrum of the NGF-0.1-900 after acidification. The appearance of the oxygen groups absorption peaks demonstrates the successful acidification of the NGF.

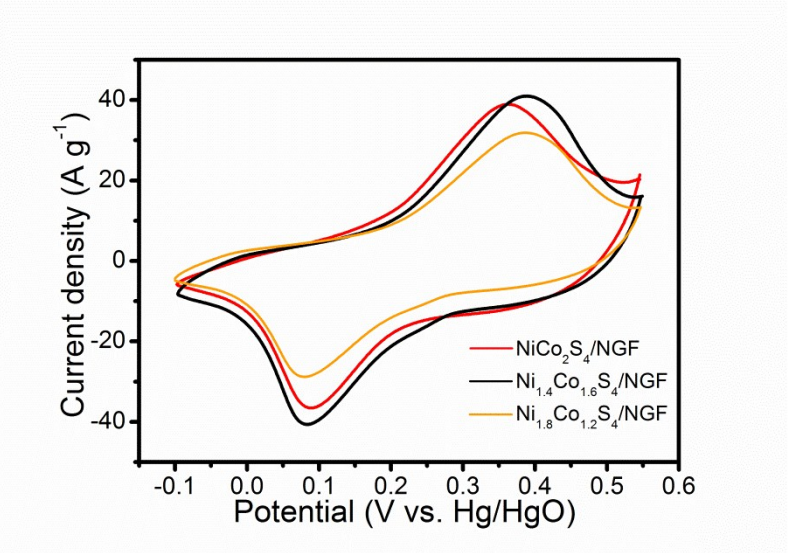

Figure S5. CV curves of the $NiCo_2S_4$/NGF, $Ni_{1.4}Co_{1.6}S_4$/NGF and $Ni_{1.8}Co_{1.2}S_4$/NGF at 10 mV s^{-1}. The highest redox peaks position along with the largest enclosed area indicate the best electrochemical performance when the molar ratio of Ni : Co is 1.4 : 1.6.

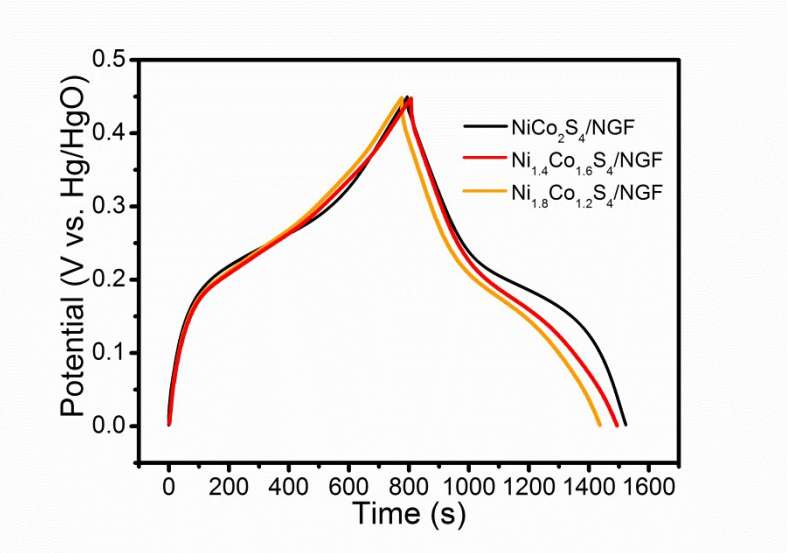

Figure S6. CP curves of the $NiCo_2S_4$/NGF, $Ni_{1.4}Co_{1.6}S_4$/NGF and $Ni_{1.8}Co_{1.2}S_4$/NGF at 1 A g^{-1}. This data indicates that the specific capacitance of the $Ni_{1.4}Co_{1.6}S_4$/NGF is the largest compared to those of the other samples on account of the longest discharge time.

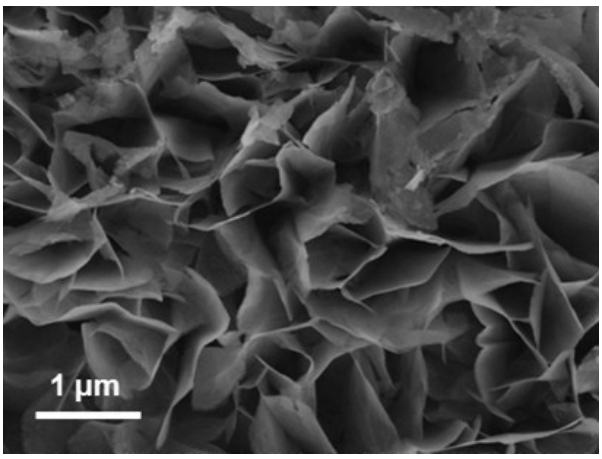

Figure S7. SEM image of the $Ni_{1.4}Co_{1.6}S_4$/NGF after galvanostatic charge/discharge at a current density of 20 A g^{-1} for 2000 cycles. The interconnected sheet-like morphology was well maintained and there only generated a small range of collapse.

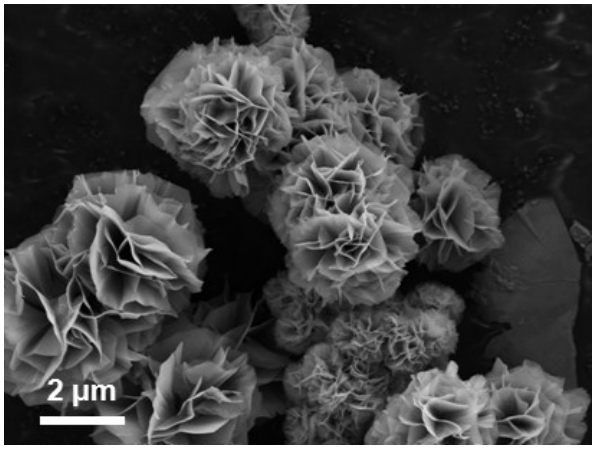

Figure S8. SEM image of the pure $Ni_{1.4}Co_{1.6}S_4$. A wide range of size distribution can be observed.

Table S1. Nitrogen contents of the NGF-0.1-800, NGF-0.1-900, and NGF-0.1-1000.

Electrode	Nitrogen content (%)		
	Graphitic-N	Pyrrolic-N	Pyridinic-N
NGF-0.1-800	10.9	89.1	0
NGF-0.1-900	65.6	12.6	21.8
NGF-0.1-1000	74.6	18.2	7.2

.

Table S2. BET specific surface area, BJH pore volume and pore diameter of the NGF-0.1-800, NGF-0.1-900, and NGF-0.1-1000.

Electrode	BET specific surface area (m^2 g^{-1})	BJH pore volume (cm^3 g^{-1})	BJH pore diameter (nm)
NGF-0.1-800	56.78	0.13	3.42
NGF-0.1-900	47.15	0.16	3.84
NGF-0.1-1000	41.42	0.17	4.17